# Fluorine containing C(60) derivatives for high-performance electron transporting field-effect transistors and integrated circuits

Wobkenberg, Paul H.; Ball, James; Bradley, Donal D. C.; Anthopoulos, Thomas D.; Kooistra, Floris; Hummelen, Jan C.; de Leeuw, Dago M.; Wöbkenberg, Paul H.

*Published in:*
Applied Physics Letters

*DOI:*
10.1063/1.2907348

# Fluorine containing $C_{60}$ derivatives for high-performance electron transporting field-effect transistors and integrated circuits

Paul H. Wöbkenberg,[1] James Ball,[1] Donal D. C. Bradley,[1] Thomas D. Anthopoulos,[1,a)]
Floris Kooistra,[2] Jan C. Hummelen,[2] and Dago M. de Leeuw[3]
[1]*Department of Physics, Blackett Laboratory, Imperial College London, London SW7 2BW, United Kingdom*
[2]*Molecular Electronics, Zernike Institute for Advanced Materials and Stratingh Institute of Chemistry, University of Groningen, Nijenborgh 4 9747 AG Groningen, The Netherlands*
[3]*Philips High-Tech Campus, Prof. Holstlaan 4 5656 AA Eindhoven, The Netherlands*

(Received 14 February 2008; accepted 17 March 2008; published online 10 April 2008)

We report on electron transporting organic transistors and integrated ring oscillators based on four different solution processible fluorine containing $C_{60}$ derivatives. Electron mobilities up to 0.15 $cm^2/V\,s$ are obtained from as-prepared bottom-gate, bottom-contact transistors utilizing gold source-drain electrodes. Despite the high mobility, no long-range structural order could be identified with the semiconductor films exhibiting amorphouslike characteristics. The good electron transport is attributed to the structural symmetry of the fullerene derivatives and the enhanced $\pi$-$\pi$ interactions between $C_{60}$ units even in the case of amorphouslike films. These advantageous characteristics make fluorine containing $C_{60}$ derivatives attractive for application in high-performance, large-area organic electronics. © *2008 American Institute of Physics*.
[DOI: 10.1063/1.2907348]

Complementary logic that combines hole transporting (*p*-channel) and electron transporting (*n*-channel) organic transistors hold promise in future large-scale integrated circuits where high manufacturing yield and good performance characteristics are required.[1] A major problem, however, associated with this approach is that *n*-channel organic semiconductors are significantly less developed when compared with their *p*-channel counterparts.[2] In addition, best performing *n*-channel molecules exhibit limited processability, hence making deposition/patterning difficult and expensive.[3,4] In order to explore alternative deposition routes, the synthesis of new molecules with enhanced electron mobility and solubility is of the outmost importance. Here we report on several solution processible fluorine (F) containing $C_{60}$ derivatives that exhibit high electron mobilities when utilized in field-effect transistors (OFETs) and unipolar (*n*-channel) circuits. Importantly, high performance is immediately obtained after spin casting of the semiconductors without the need of any additional annealing or postprocessing steps. This property makes fullerene derivatives strong candidates for applications in high performance, low-cost, and large area electronics.

The effect of incorporating F containing groups for the stabilization of electron transport in organic semiconductors is well documented in the literature.[5–8] Here, a similar strategy has been adopted for the development of soluble fullerene derivatives. The molecular structures of the four derivatives synthesized and studied are shown in Fig. 1. Synthesis of compound 1 was performed by a Prato reaction[9] where $C_{60}$ was allowed to react with sarcosine and commercially available 4-(4,4,5,5,6,6,7,7,8,8,9,9,10,10,11,11,11heptadeca-fluoroundecyloxy)benzaldehyde. Fullerene derivatives 2 and 3 were synthesized using a route similar to the one reported earlier for [6,6]-phenyl-C61-butyric acid methyl ester ([60]PCBM).[10] In brief, benzoylbutyric acid was esterified with the appropriate alcohols. The obtained ketoesters were then subjected to a condensation reaction with *p*-tosylhydrazide forming the desired tosylhydrazones. Subsequently, the tosylhydrazones were transformed *in situ* to the active diazo species which underwent a 1,3-dipolar addition reaction with a C=C bond of $C_{60}$, obtaining the desired fluorine containing fullerene derivatives 2 and 3. Finally, the synthesis of compound 4 has been described in detail elsewhere.[11]

To study but also compare the electronic structure of the four $C_{60}$ derivatives, cyclic voltammetry (CV), differential pulse voltammetry (DPV), and ultraviolet-visible (UV-vis) absorption measurements were performed. Experimental conditions for CV and DPV were potential versus $Fc/Fc^+$ (ferrocene/ferricinium), tetrabutylammonium hexafluorophosphate ($Bu_4NPF_6$, 0.1 M) as the supporting electrolyte, 1,2,-dichlorobenzene (ODCB)/acetonitrile (ODCB:MeCN-4:1) as the solvent and 10 mV/s scan rate. The working and counterelectrodes were Pt wires while the reference electrode

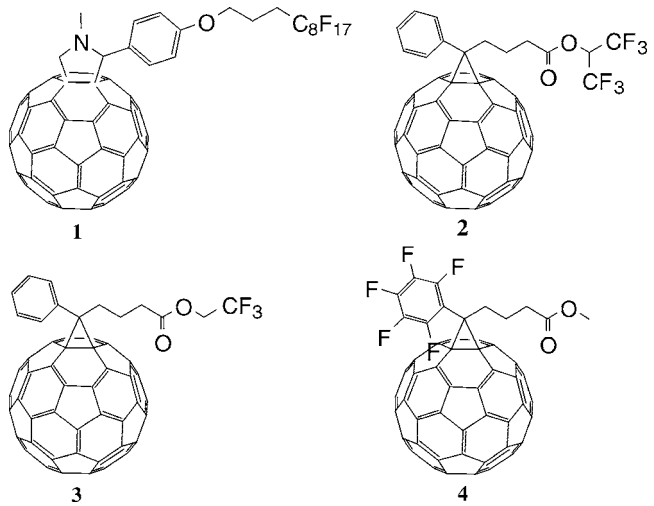


FIG. 1. Chemical structures of the fluorine containing fullerene derivatives 1–4.

a)Author to whom correspondence should be addressed. Electronic mail: thomas.anthopoulos@imperial.ac.uk.

 

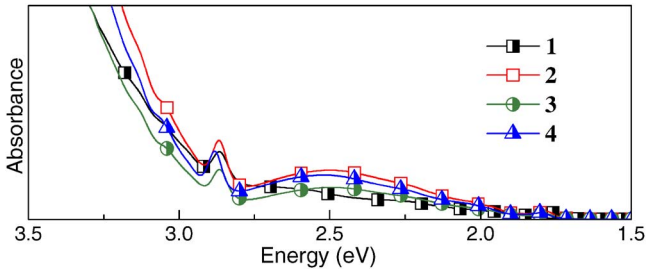


FIG. 2. (Color online) UV-vis absorption spectra of the fluorine containing fullerene derivatives 1–4 in solution.

TABLE I. Performance parameters of transistors based on fullerene derivatives 1–4.

| | $\mu$ ($cm^2$/V s) | | On/off current ratio ($\times 10^4$) | | $V_{TH}$ (V) | |
|---|---|---|---|---|---|---|
| Fullerene | Type I | Type II | Type I | Type II | Type I | Type II |
| 1 | 0.1 | 0.15 | 2.1 | >100 | 21 | 12 |
| 2 | 0.08 | 0.06 | 8.4 | >10 | 27 | 30 |
| 3 | 0.08 | 0.08 | 3.4 | >10 | 10 | 10 |
| 4 | 0.02 | 0.03 | 1.3 | >10 | 25 | 20 |

was an Ag wire. Electrochemical characterization of derivatives 1–4 reveals highly reversible first, second, and third reduction peaks (data not shown). The first reduction potentials for all four molecules are similar with values ranging between −1.042 to −1.098 V. The UV-vis absorption spectra of 1–4, in solution, also show great similarities (Fig. 2). Analysis of the data yields an estimate of the optical bandgap in the range of 1.6–1.8 eV. By combining the latter with the first reduction potentials and assuming an exciton binding energy of 0.3–0.5 eV, approximate values for the lowest unoccupied molecular orbitals (LUMO) and highest occupied molecular orbital levels for each compound were calculated yielding 3.5–3.8 and 5.7–6.1 eV, respectively.

To assess the suitability of 1–4 as *n*-channel semiconductors in OFETs, two different device architectures were investigated. Type I transistors, with $L=60$ $\mu$m and $W=1$ mm, were fabricated in a bottom-gate, top-contact configuration employing glass substrates coated with indium tin oxide as the gate electrode. Divinyltetramethyldisiloxane-bis(benzocyclobutene) (BCB) was employed as gate dielectric with a geometrical capacitance of $C_i=1.5$ nF/$cm^2$. Compounds 1–4 were then spun from chlorobenzene solutions (10 mg/ml wt. %) at room temperature in $N_2$ ambient. Device fabrication was completed by the evaporation of Ca source-drain (S-D) electrodes in high vacuum ($10^{-6}$ mbar) through shadow masks. Type II transistors with $L=10$ $\mu$m and $W=20$ mm, were fabricated in a bottom-contact, bottom-gate configuration using highly doped Si and $SiO_2$ as the gate electrode and gate dielectric ($C_i=17$ nF/$cm^2$), respectively, employing photolithographically defined gold (Au) S-D electrodes. The $SiO_2$ layer was treated with the primer hexamethyldisilazane (HMDS) prior to semiconductor depostition. For the fabrication of the seven-stage ring oscillators type II transistors were employed. Gate electrodes and first-level interconnect lines were made by patterning the gold layer using standard photolithography techniques. The gate dielectric was a 300 nm thick photoimageable polymer (polyvinylphenol), which was spin coated and subsequently exposed to ultraviolet light to define contact holes (vias). Source and drain electrodes and second level interconnects were defined in the second gold layer. The specific circuit design employed is based on the ratio logic[12] with the driver/load transistor ratio set to 8. The widths of the driver, load, and buffer transistors were 2, 0.25, and 5 mm, respectively. The channel length for all transistors was kept constant and equal to 1.5 $\mu$m. Finally, circuit fabrication was completed with the spin coating of the semiconductor at 1000 rpm for 60 s. Fabrication and electrical characterization was performed at room temperature under $N_2$.

Figure 3(a) illustrates the output curves for a type I OFET (see inset) based on 1. The linearity of the curves at low $V_D$ indicates Ohmic-like injection behavior. Moreover, the device exhibit negligible hysteresis, a sign of trap-free electron transport. Similar operating characteristics are observed for OFETs based on compounds 2–4. Figure 3(b) displays the output curves for a type II OFET (see inset) based on 1. Unlike type I devices, the output curves show strong injection-limited characteristics as evident from the superlinear dependence of $I_D$ on $V_D$ at low bias. The latter is attributed to the significant energy offset (1.2–1.5 eV) between the Fermi level of Au and the LUMO energy of 1. The performance characteristics of type I and type II OFETs based on 1–4 are summarized in Table I.

Despite the significant barrier for injection, type II transistors based on 1 yield the highest electron mobility (0.15 $cm^2$/V s). This result can be attributed either to a smoother $SiO_2$-HMDS surface, as compared to BCB, or to its surface energy characteristics. To investigate this further we carried atomic force microscopy (AFM) and contact angle measurements on both $SiO_2$-HMDS and BCB surfaces. Interestingly, AFM measurements suggest that the BCB surface is smoother (rms ~1.18 nm) than that of $SiO_2$-HMDS (rms ~2.2 nm). Hence, the high electron mobility obtained from type II transistors cannot be attributed to the flatness of

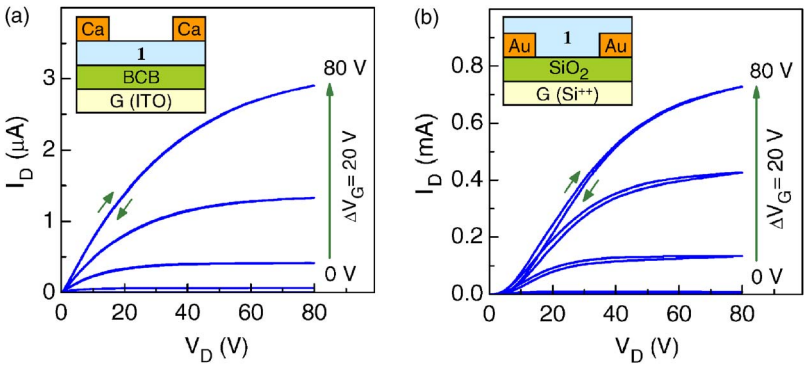


FIG. 3. (Color online) Output characteristics for a type I (a) and a type II (b) transistors based on 1. The channel dimensions for the type I device are $L=60$ $\mu$m and $W=1$ mm. For the type II transistor $L=10$ $\mu$m, $W=20$ mm. Insets: schematic structures of type I (a) and type II (b) transistors tested.

the $SiO_2$-HMDS surface. Contact angle measurements, on other hand, show that the BCB surface is characterized by a low polar component (0.22 mN/m) and a very high dispersive component (36.54 mN/m) as compared to $SiO_2$-HMDS (25.3 and 20.9 mN/m, respectively). Furthermore, from surface tension measurements on pendant drops the polar and dispersive component of derivative 1 in chlorobenzene solution were also calculated yielding 2.81 and 21.65 mN/m, respectively. Since both BCB and $SiO_2$-HMDS surfaces are found to wet equally well (contact angles $<4°$), one could argue that the interaction between the organic solution based on derivative 1 and the substrates is governed by dispersive forces. Therefore, a possible explanation for the lower electron mobilities obtained from type I OFETs is the stronger interaction between the organic semiconductor and the BCB surface.

Compounds 2 and 3 show slightly lower mobilities with compound 4 exhibiting the lowest value. We note that upon annealing all transistors show a reduction in the electron mobility by a factor of 2–3. The origin of this effect is not yet understood. The most important finding associated with the as-prepared transistors is that performance appears to be unaffected by the scaling down of the channel length (i.e., 60–10 $\mu$m) but also by the use of gold S-D electrodes in conjunction with the more technologically relevant bottom-gate, bottom-contact device architecture. To demonstrate the importance of these key advantages in real circuit applications we have fabricated a number of unipolar multistage ring oscillators. Figure 4(a) displays a micrograph of the actual seven-stage ring oscillator circuit based on type II OFETs employing $L=1.5$ $\mu$m as the design rule. The oscillation frequency ($f_{osc}$) of the oscillator based on derivative 1 versus the applied voltage ($V_{DD}$) is displayed in Fig. 4(b). The inset shows the output signal obtained at $V_{DD}=170$ V. The maximum $f_{osc}$ measured is 10.4 kHz and corresponds to a stage delay of $\tau=6.86$ $\mu$s ($\tau=1/[2\times n\times f_{osc}]$, where $n$ is the number of inverting stages). Despite the short channel dimensions (i.e., $L=1.5$ $\mu$m) and the use of Au electrodes, the present circuit is the fastest solution processed $n$-type ring oscillator reported to date.

In order to gain an insight into the structural properties of 1–4 films, x-ray diffraction measurements were carried out in a reflection mode under ambient conditions. For this purpose, fullerene films were spun on $Si/SiO_2$ substrates. Surprisingly, and despite repeated attempts, no scattering intensities could be recorded suggesting the absence of any significant macroscopic order. Taking this into consideration the high electron mobilities obtained here could be ascribed to the molecular symmetry of the fullerene derivatives and the strong $\pi$-$\pi$ interactions between neighboring $C_{60}$ units even in the case of amorphouslike films. The present findings highlight the advantages of soluble F containing fullerenes for low-cost electronic applications.

Finally, few additional advantages associated with the F containing 1–4 derivatives reported in this study is the improved stability toward atmospheric air as well as the useful solvent orthogonality. For example, we are able to fabricate high mobility (0.1 $cm^2/V$ s) top-gate OFETs based on 1 with shelve lifetime of few days. This greatly enhanced stability, as compared to standard methanofullerene OFETs,[12,13] is attributed to the F atoms and their tendency to repeal water. The latter is believed to be the main atmospheric oxidant responsible for the $n$-channel degradation in OFETs.[14] Further work on device stability is currently underway and will be reported in the future.

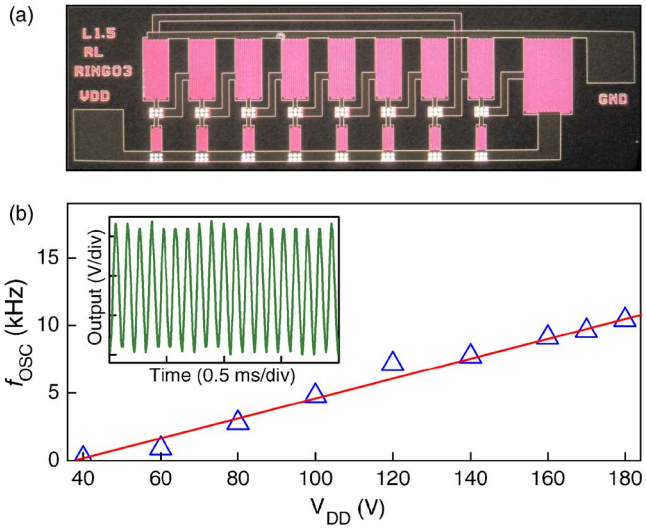


FIG. 4. (Color online) (a) Micrograph of the seven-stage ring oscillator based on type II transistors employing $L=1.5$ $\mu$m as the design rule. (b) Oscillation frequency vs $V_{DD}$ for a seven-stage ring oscillator based on 1. Inset: output signal at $V_{DD}=170$ V.

In summary, high mobility $n$-channel OFETs and unipolar seven-stage ring oscillators based on a number of fluorine containing fullerene derivatives have been demonstrated. Despite the high performance we were unable to identify any long-range order in the film structure. The latter makes F containing fullerene derivatives attractive for use in low-cost, large area organic electronics.

We are grateful to the Engineering and Physical Sciences Research council (EPSRC) for financial support. T.D.A. is an EPSRC Advanced Research Fellow.

[1] B. K. Crone, A. Dodabalapur, Y.-Y. Lin, R. W. Fillas, Z. Bao, A. LaDuca, R. Sarpeshkar, H. E. Katz, and W. Li, Nature (London) **403**, 521 (2000).
[2] J. Zaumseil and H. Sirringhaus, Chem. Rev. (Washington, D.C.) **107**, 1296 (2007).
[3] M. L. Chabinyc and A. Salleo, Chem. Mater. **16**, 4509 (2004).
[4] H. E. Katz, Chem. Mater. **16**, 4748 (2004).
[5] H. E. Katz, A. J. Lovinger, J. Johnson, C. Kloc, T. Siegrist, W. Li, Y.-Y. Lin, and A. Dodabalapur, Nature (London) **404**, 478 (2000).
[6] Z. Bao, A. J. Lovinger, and J. Brown, J. Am. Chem. Soc. **120**, 207 (1998).
[7] S. Ando, R. Murakami, J.-I. Nishida, H. Tada, Y. Inoue, S. Tokito, and Y. J. Yamashita, J. Am. Chem. Soc. **127**, 14996 (2005).
[8] A. Facchetti, M. Mushrush, H. E. Katz, and T. J. Marks, Adv. Mater. (Weinheim, Ger.) **15**, 33 (2003).
[9] M. Prato and M. Maggini, Acc. Chem. Res. **31**, 519 (1998).
[10] J. C. Hummelen, B. W. Knight, F. LePeq, F. Wudl, J. Yao, and C. L. J. Wilkins, Org. Chem. **60**, 532 (1995).
[11] F. B. Kooistra, J. Knol, F. Kastenberg, L. M. Popescu, W. J. H. Verhees, J. M. Kroon, and J. C. Hummelen, Org. Lett. **9**, 551 (2007).
[12] T. D. Anthopoulos, D. M. de Leeuw, E. Cantatore, P. van't Hof, J. Alma, and J. C. Hummelen, J. Appl. Phys. **98**, 054503 (2005).
[13] T. D. Anthopoulos, C. Tanase, S. Setayesh, E. J. Meijer, J. C. Hummelen, P. W. Blom, and D. M. de Leeuw, Adv. Mater. (Weinheim, Ger.) **16**, 2174 (2004).
[14] T. D. Anthopoulos, G. C. Anyfantis, G. C. Papavassiliou, and D. M. de Leeuw, Appl. Phys. Lett. **90**, 122105 (2007).